

FINDING A WEAK SOLUTION OF THE HEAT DIFFUSION DIFFERENTIAL EQUATION FOR TURBULENT FLOW BY GALERKIN'S VARIATION METHOD USING P-VERSION FINITE ELEMENTS

I. PÁCZELT

Institute of Applied Mechanics, University of Miskolc
3515 Miskolc-Egyetemváros, Hungary

Istvan.Paczelt@uni-miskolc.hu

[Received: September 29, 2021; Accepted: November 11, 2021]

Dedicated to Professor Tibor Czibere on the occasion of his 90th birthday

Abstract. The stochastic turbulence model developed by Professor Czibere provides a means of clarifying the flow conditions in pipes and of describing the heat evolution caused by shear stresses in the fluid. An important part of the theory is a consideration of the heat transfer-diffusion caused by heat generation. Most of the heat is generated around the pipe wall. One part of the heat enters its environment through the wall of the tube (heat transfer), the other part spreads in the form of diffusion in the liquid, increasing its temperature. The heat conduction differential equation related to the model contains the characteristics describing the turbulent flow, which decisively influence the resulting temperature field, appear. A weak solution of the boundary value problem is provided by Bubnov-Galerkin's variational principle. The axially symmetric domain analyzed is discretized by a geometrically graded mesh of a high degree of p-version finite elements, this method is capable of describing substantial changes in the temperature gradient in the boundary layer. The novelty of this paper is the application of the p-version finite element method to the heat diffusion problem using Czibere's turbulence model. Since the material properties depend on temperature, the problem is nonlinear, therefore its solution can be obtained by iteration. The temperature states of the pipes are analyzed for a variety of technical parameters, and useful suggestions are proposed for engineering designs.

Mathematical Subject Classification: 76F10, 80A19, 65N30

Keywords: Stochastic turbulent flow model, heat diffusion problem, Galerkin method, p-version finite elements

1. INTRODUCTION

In short, the calculation of turbulent flow in a long straight pipe based on the stochastic turbulence model [1–3] will be summarized. In this model, the mechanical similarity hypothesis was successfully extended to a three-dimensional turbulent flow by confirming it with experimental results. The model is suitable for investigating steady-state turbulent flow. An important result is the introduction of the eddy viscosity tensor \mathbf{G} instead of the Bousinesq scalar vortex viscosity factor, as well as an extended interpretation of Prandtl's length scale l_{\max} . The latter could be derived using the known dimensional analysis: ($l = l_{\max}/\kappa$). Here l is the length scale of turbulence, and κ is the Kármán constant.

This paper does not aim to critically analyze different turbulence models [4–11]. Here, we focus primarily on the approximate solution of the thermal conduction problem related to Czibere’s turbulence model.

1.1. Fundamental assumptions. For an incompressible fluid flow in the stochastic turbulence model, the governing equations of the transport of mass, momentum, internal energy and the turbulent kinetic energy equation are written in direct notation:

$$\nabla \cdot \mathbf{v} = 0, \quad (1)$$

$$\rho \left(\frac{\partial \mathbf{v}}{\partial t} + (\mathbf{v} \cdot \nabla) \mathbf{v} \right) = \rho \mathbf{g} - \nabla \mathbf{p} - \frac{2}{3} \rho \nabla k + \eta \Delta \mathbf{v} + \text{Div}(\Theta \mathbf{G}) \quad (2)$$

$$\rho c_p \left(\frac{\partial T}{\partial t} + (\mathbf{v} \cdot \nabla) T \right) = \nabla \cdot [(\lambda + \Lambda) \nabla T] + \rho(\varphi_D + \varepsilon) \quad (3a)$$

$$\rho \left(\frac{\partial k}{\partial t} + (\mathbf{v} \cdot \nabla) k \right) = \Theta \mathbf{G} : (\nabla \circ \mathbf{v}) - \rho \varepsilon - \nabla \cdot \left\{ \frac{\Theta^{3/2} \mathbf{t}}{2\rho^{1/2} \kappa^3} - \frac{C_k}{\kappa \Omega} (\Theta \rho k)^{1/2} \right\} + v \left[\frac{5}{3} \rho \Delta k - \nabla \cdot \text{Div}(\Theta \mathbf{G}) \right], \quad (3b)$$

where the interpretation of the different quantities can be found in the Nomenclature. In addition, \mathbf{H} and \mathbf{H}_* are the similarity tensor and its deviator of the stochastic turbulence model, respectively:

$$\mathbf{H} = \begin{pmatrix} \alpha & 1 & 0 \\ 1 & \beta & 0 \\ 0 & 0 & \gamma \end{pmatrix}, \quad \mathbf{H}_* = \begin{pmatrix} \alpha_* & 1 & 0 \\ 1 & \beta_* & 0 \\ 0 & 0 & \gamma_* \end{pmatrix}; \quad \begin{aligned} \alpha_* &= \frac{1}{3}(2\alpha - \beta - \gamma) \\ \beta_* &= \frac{1}{3}(2\beta - \alpha - \gamma) \\ \gamma_* &= \frac{1}{3}(2\gamma - \alpha - \beta) \end{aligned}$$

where $a^2 = -\frac{1}{2}(\alpha + \beta + \gamma)$, $\alpha = -3.28$, $\beta = -1.64$, $\gamma = -2.46 \times v$ are the three entries of these tensors, according to Prandtl parameter $C_k \leq 1$. Naturally, for fully-developed turbulent flows, the terms of the time derivatives are omitted in equations (2) and (3). \mathbf{G} , the eddy viscosity tensor, is also defined as $\mathbf{G} = \mathbf{E} \cdot \mathbf{H}_* \cdot \mathbf{E}^T$, where $\mathbf{E} = [E_{ij}]$ is the tensor of the transformation between the natural and the reference coordinate systems, with $\mathbf{E}^T = [E_{ji}]$ being its transpose. The elements of the transformation tensor \mathbf{E} are given as:

$$E_{i1} = \frac{1}{\sqrt{1 - S^2}} \left(\frac{v_i}{v} - S \frac{\Omega_i}{\Omega} \right), \quad E_{i2} = \frac{1}{\sqrt{1 - S^2}} \left(\frac{v_{i+1} \Omega_{i+2} - v_{i+2} \Omega_{i+1}}{v \Omega} \right), \quad E_{i3} = -\frac{\Omega_i}{\Omega}$$

$$v = \sqrt{v_1^2 + v_2^2 + v_3^2}, \quad \Omega = \sqrt{\Omega_1^2 + \Omega_2^2 + \Omega_3^2}, \quad S = \frac{1}{\sqrt{1 - S^2}} \left(\frac{v_1 \Omega_1 + v_2 \Omega_2 + v_3 \Omega_3}{v \Omega} \right),$$

$$i = 1, 2, 3$$

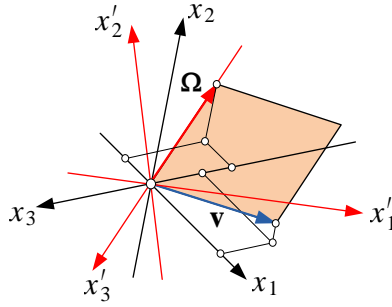


Figure 1. Natural x'_1, x'_2, x'_3 and reference x_1, x_2, x_3 coordinate systems [1]

The base vectors of the natural coordinate system are defined by the velocity \mathbf{v} and vortex velocity vector $\mathbf{\Omega} = \nabla \times \mathbf{v}$:

$$\mathbf{e}'_2 = \frac{\mathbf{v} \times \mathbf{\Omega}}{|\mathbf{v} \times \mathbf{\Omega}|}, \quad \mathbf{e}'_3 = -\frac{\mathbf{\Omega}}{\Omega} = -\frac{\nabla \times \mathbf{v}}{|\nabla \times \mathbf{v}|}, \quad \mathbf{e}'_1 = \mathbf{e}'_2 \times \mathbf{e}'_3.$$

Equations (1) to (3) consist of a total of five scalar differential equations. In this differential equation system there are six unknown functions: $(v_1, v_2, v_3, p, T, \Theta)$, therefore the system (1)-(3) is underdetermined, that is, it needs to be supplemented with one equation.

The additional differential equation is created considering the following assumptions. Using the definition of the specific turbulent dissipation

$$\varepsilon = v \overline{(\mathbf{v}' \circ \nabla) : (\mathbf{v}' \circ \nabla + \nabla \circ \mathbf{v}')}$$

in case of stochastic turbulence it is written as [1]:

$$\varepsilon = -v\kappa^2 [a_{11}A_1^2 + a_{22}A_2^2 + a_{33}A_3^2 + 2(a_{12}A_1A_2 + a_{13}A_1A_3 + a_{23}A_2A_3)],$$

where \mathbf{v}' is fluctuation of the velocity, and $\bar{(\cdot)}$ is the time-average value,

$$\begin{aligned} a_{11} &= 2\alpha + \beta + \gamma, & a_{22} &= \alpha + 2\beta + \gamma, & a_{33} &= \alpha + \beta + 2\gamma, \\ a_{12} &= \alpha + \beta + \gamma + 1, & a_{13} &= \alpha + \beta + \gamma, & a_{23} &= \alpha + \beta + \gamma, \end{aligned}$$

$$A_i = \frac{1}{2\kappa(\rho\Theta)^{1/2}} \left[E_{i1} \frac{\partial\Theta}{h_1\partial x_1} + E_{i2} \frac{\partial\Theta}{h_2\partial x_2} + E_{i3} \frac{\partial\Theta}{h_3\partial x_3} \right], \quad i = 1, 2, 3.$$

The π theorem of dimensional analysis states that every physical process can be outlined by a relationship between a certain number of dimensionless characteristics. The process of turbulent fluctuation is fundamentally determined by the length scale l , the absolute value of the vortex vector $\mathbf{\Omega}$, the specific turbulent dissipation ε , and the kinematic viscosity ν of the medium [1]. In view of the above, with the help of the π theory of dimension analysis, the specific turbulent dissipation ε takes the form of

$$\varepsilon = C_E \nu^N \frac{\Omega^{N-1}}{(\Omega)^{2(N-1)}} = C_E \kappa^{2(N-1)} \frac{\eta^N}{\rho} \frac{\Omega^{N-1}}{\Theta^{N-1}},$$

where $1 < N < 3$ and C_E is a suitably chosen coefficient. The additional differential equation is obtained by combining the two equations for ε :

$$\begin{aligned} a_{11}A_1^2 + a_{22}A_2^2 + a_{33}A_3^2 + 2(a_{12}A_1A_2 + a_{13}A_1A_3 + a_{23}A_2A_3) = \\ = -C_E\kappa^{2(N-2)}\eta^{N-1}\frac{\Omega^{N-1}}{\Theta^{N-1}}. \end{aligned} \quad (4)$$

As there is no unknown function in this differential equation, it is a good candidate for supplementing the underdetermined system of differential equations (1) to (3), forming a *one-equation* version of the stochastic turbulence model.

The following will address axisymmetric problems for a steady-state turbulent flow, that is the problems are time-independent.

In the case of fluid flow in a long straight pipe, in the x_1, x_2, x_3 coordinate system, only the velocity component v_1 depends on the radial coordinate x_2 , and it is different from zero. In this case, the turbulence length scale l varies only in the radial direction, and consequently the dominant turbulent shear stress Θ and the turbulent kinetic energy k also depend only on radial direction: i.e., $\Theta(x_2)$ and $k(x_2)$. However, pressure and temperature depend on two coordinates: i.e., $p(x_1, x_2)$, $T(x_1, x_2)$. After that, the vortex components are given as follows:

$$\Omega_1 = \Omega_2 = 0, \quad \Omega_3 = -\frac{dv_1}{dx_2}.$$

Entries of tensor \mathbf{E} transforming between the natural and reference coordinate systems are given as:

$$\begin{array}{lll} E_{11} = 1, & E_{12} = 0, & E_{13} = 0, \\ E_{21} = 0, & E_{22} = -1, & E_{23} = 0, \\ E_{31} = 0, & E_{32} = 0, & E_{33} = -1. \end{array}$$

The entries of the vortex viscosity tensor \mathbf{G} are as follows:

$$\begin{array}{lll} G_{11} = \alpha_*, & G_{22} = \beta_*, & G_{33} = \gamma_* \\ G_{12} = G_{21} = -1, & G_{13} = G_{31} = G_{23} = G_{32} = 0. \end{array}$$

This means that in the case of fluid flow in a long straight pipe, the continuity equation (1) is automatically satisfied; and the equation of linear momentum (2) develops in this way by neglecting the gravity force in axial direction:

$$0 = -\frac{\partial p}{\partial x_1} + \eta \left(\frac{d^2 v_1}{dx_2^2} + \frac{1}{x_2} \frac{dv_1}{dx_2} \right) - \frac{d\Theta}{dx_2} - \frac{\Theta}{x_2} \quad (5a)$$

in radial direction:

$$0 = -\frac{\partial p}{\partial x_2} + \left(\beta_* - \frac{2a^2}{3} \right) \frac{d\Theta}{dx_2} + \frac{\Theta}{x_2} (\beta_* - \gamma_*) \quad (5b)$$

Deriving (5a) with respect to x_1 , $\frac{\partial^2 p}{\partial x_1^2} = 0$ is obtained for the pressure p , and its solution is given as $p(x_1, x_2) = A(x_2) + Bx_1$, where constant B can be calculated by a pressure drop $\Delta p = p_1 - p_2$, which is measured in length L of the pipe $B = -\frac{\Delta p}{L}$,

$p_1 = p(0, x_2)$, $p_2 = p_2(L, x_2)$. Then the momentum equations (5a) and (5b) can be written in the following form:

$$\eta \left(\frac{d^2 v_1}{dx_2} + \frac{1}{x_2} \frac{dv_1}{dx_2} \right) - \frac{d\Theta}{dx_2} - \frac{\Theta}{x_2} = -\frac{\Delta p}{L}, \tag{6a}$$

$$\left(\beta_* - \frac{2a^2}{3} \right) \frac{d\Theta}{dx_2} + \frac{\Theta}{x_2} (\beta_* - \gamma_*) = f'(x_2). \tag{6b}$$

Equation (6a) can be reshaped as follows:

$$\eta \frac{d}{dx_2} \left(x_2 \frac{dx_1}{dx_2} \right) - \frac{d}{dx_2} (x_2 \Theta) = -\frac{\Delta p}{L} x_2.$$

This equation is integrated with respect to x_2 , and the result is divided by x_2 :

$$\eta \frac{dv_1}{dx_2} - \Theta = -\frac{\Delta p}{2L} x_2 + \frac{C}{x_2}.$$

Taking into account that in the middle of the pipe (where $x_2 = 0$) neither dv_1/dx_2 nor the dominant turbulent shear stress Θ can be infinitely high, the integration constant C is zero. Thus the momentum equation (6a) is finally written as follows:

$$\eta \frac{dv_1}{dx_2} - \Theta = -\frac{\Delta p}{2L} x_2 \tag{7}$$

In the case of fluid flow in a long straight pipe, the parameters A_i of equation (4) are given as follows:

$$A_1 = 0, \quad A_2 = -\frac{1}{2\kappa(\rho\Theta)^{1/2}} \frac{d\Theta}{dx_2}, \quad A_3 = 0.$$

Finally, equation (4) takes the form of:

$$\frac{a_{22}}{4\kappa^2 \rho \Theta} \left(\frac{d\Theta}{dx_2} \right)^2 = -C_E \kappa^{2(N-2)} \eta^{N-1} \frac{\Omega^{N+1}}{\Theta^{N-1}}$$

After some manipulations we have the following form:

$$\Theta^{\frac{N-2}{2}} \frac{d\Theta}{dx_2} = 2\rho^{\frac{N}{2}} \left(-\frac{C_E v^{N-1}}{\alpha + 2\beta + \gamma} \right)^{1/2} \kappa^{N-1} \Omega^{\frac{N+1}{2}}. \tag{8}$$

It is easy to see that from the point of view of determining the unknown functions v_1 and Θ , differential equations (7) and (8) form a closed system. By solving them, the functions can be numerically determined.

1.2. Preparation for numerical computations. Numerical computations are performed with dimensionless physical variables. The dimensionless counterpart of velocity v_1 is the wall friction velocity v_* , which is defined by the viscous shear stress on the wall $\tau(R_0)$. The wall friction velocity is obtained as:

$$\rho v_*^2 = |\tau R_0| = \eta \left| \frac{dv_1}{dx_2} \right|_{x_2=R_0} = \frac{\Delta p R_0}{2L}, \quad v_* = \sqrt{\frac{\Delta p R_0}{\rho 2L}},$$

where R_0 is the inner radius of the pipe. The modified Reynolds number is calculated with the wall friction velocity v_* : $Re_* = v_* R_0 / \nu$.

Introducing the following notations

$$\xi = \frac{x_2}{R_0}, \quad V(\xi) = \frac{v_1}{v_*}, \quad H(\xi) = \frac{\Theta}{\rho v_*^2}$$

the momentum transport equation (7) takes the form of

$$\frac{dV}{d\xi} = \text{Re}_*(H - \xi). \quad (9a)$$

Using the dimensionless parameters in differential equation (7) and substituting them into equation (9a), the following differential equation is obtained:

$$\frac{dH}{d\xi} = C_H \sqrt{\frac{|H - \xi|^{N+1}}{H^{N-2}}}, C_H = 2\kappa^{N-1} \text{Re}_* \sqrt{-\frac{C_E}{\alpha + 2\beta + \gamma}} \quad (9b)$$

where coefficient C_H from the numerical experiment is [3]:

$$C_H = 0.157 \text{Re}_*^{1.528} \quad \text{for } \text{Re}_* < 1134, \quad C_H = 1.125 \text{Re}_*^{1.248} \quad \text{for } 1134 < \text{Re}_* < 21553,$$

$$C_H = 446 \text{Re}_*^{0.418} \quad \text{for } 21553 < \text{Re}_*$$

By solving the closed system of differential equations (9a) and (9b), the functions $V(\xi)$ and $H(\xi)$ can be numerically determined. The boundary conditions at $\xi = 0$ are defined as:

$$H(0) = 0, \quad V(0) = \frac{v_m}{v_*} = \frac{1}{\kappa} \ln \text{Re}_* + 6.0,$$

where v_m is the velocity maximum [3]. Differential equations (9a) and (9b) are solved by the Runge-Kutta method.

For fluid flows in pipes, the relationship between the Reynolds number Re and its modified value Re_* is written as $\text{Re}_* = \sqrt{\frac{f}{2}} \frac{\text{Re}}{4}$, where

$$\text{Re} = \frac{2v_a R_0}{\nu} \frac{1}{\sqrt{f}} = \frac{1}{2\kappa\sqrt{2}} \ln \left(\text{Re} \sqrt{f} \right) - 0.8. \quad (10)$$

Here v_a is the average velocity in the pipe section, f is the friction factor in the fluid flow.

Differential equations (9a) and (9b), like the turbulence model itself, are based on the already fully formed turbulence condition. They lose their validity in the viscous boundary layer along the wall because the presence of the wall attenuates the development of turbulence. Therefore, the slowing effect of the wall on the turbulence in the pipe flow is represented by the following damping function $\tilde{D}(\xi)$:

$$\tilde{D}(\xi) = \exp \left(\frac{b\xi}{\xi - 1} \right), \quad b = \frac{3}{\text{Re}_*}.$$

Multiplying the solution of differential equation (9b) by this damping function, the result satisfies also the boundary condition $H(1) = 0$. Then differential equation (9a) is solved with the attenuated distribution $H(\xi)$ to determine the function $V(\xi)$. In order to satisfy the condition $V(1) = 0$, differential equation (9a) is solved with the

help of the following multiplicative cutoff function, which makes the solution smooth in the vicinity of the wall:

$$Y(\xi) = (\tilde{A}_1\xi + \tilde{A}_0)(\xi - 1), \xi_\delta \leq \xi \leq 1$$

where $\xi_\delta = 1 - 3/\text{Re}_*$ denotes the location of the fitting; and the coefficients \tilde{A}_1 and \tilde{A}_0 can be calculated as follows:

$$\tilde{A}_1 = \frac{V'(\xi_\delta)}{\xi_\delta - 1} - \frac{V(\xi_\delta)}{(\xi_\delta - 1)^2}, \quad A_0 = V'(\xi_\delta) - (2\xi_\delta - 1)\tilde{A}_1$$

In case of stationary flow in a long straight pipe, using the divergence of the vector function $\mathbf{f}(r)$:

$$\nabla \cdot \mathbf{f} = \frac{1}{h_1 h_2 h_3} \left(\frac{\partial}{\partial x_1} (f_1 h_2 h_3) + \frac{\partial}{\partial x_2} (f_2 h_3 h_1) + \frac{\partial}{\partial x_3} (f_3 h_1 h_2) \right)$$

and taking into account that $h_1 = h_2 = 1$ and $h_3 = x_2$ the transport equation for internal energy (3) will have the form

$$\rho c_p v_1 \frac{\partial T}{\partial x_1} = \frac{\partial}{\partial x_1} \left[(\lambda + \Lambda) \frac{\partial T}{\partial x_1} \right] + \frac{\partial}{\partial x_2} \left[(\lambda + \Lambda) \frac{\partial T}{\partial x_2} \right] + \frac{1}{x_2} (\lambda + \Lambda) \frac{\partial T}{\partial x_2} + \rho (\varphi_D + \varepsilon), \quad (11a)$$

where the viscous and turbulent dissipations φ_D and ε are given by the expressions

$$\varphi_D = v \left(\frac{dv_1}{dx_2} \right)^2, \quad \varepsilon = -v \frac{a_{22}}{4\rho\Theta} \left(\frac{d\Theta}{dx_2} \right)^2.$$

Let us introduce dimensionless location coordinates $s = x_1/R_0$, $\xi = x_2/R_0$ and dimensionless variables

$$\varphi = \frac{R_0 \varphi_D}{v_*^3} = \frac{1}{\text{Re}_*} \left(\frac{dV}{d\xi} \right)^2, \quad \psi = \frac{R_0 \varepsilon}{v_*^3} = -\frac{\alpha + 2\beta + \gamma}{4\text{Re}_* H} \left(\frac{dH}{d\xi} \right)^2, \quad \vartheta = \frac{T}{T_0},$$

where T_0 is the reference temperature.

The former transport equation of internal energy (11a) with the dimensionless coordinates and variables is formed as

$$\text{Pr Re}_* V(\xi) \frac{d\vartheta}{ds} = \frac{1}{\lambda} \left[\frac{\partial \lambda}{\partial s} \left(1 + \frac{\Lambda}{\lambda} \right) \frac{\partial \vartheta}{\partial s} \right] + \frac{1}{\lambda} \left[\frac{\partial \lambda}{\partial \xi} \left(1 + \frac{\Lambda}{\lambda} \right) \frac{\partial \vartheta}{\partial \xi} \right] + \frac{\partial}{\partial s} \left[\left(1 + \frac{\Lambda}{\lambda} \right) \frac{\partial \vartheta}{\partial s} \right] + \frac{\partial}{\partial \xi} \left[\left(1 + \frac{\Lambda}{\lambda} \right) \frac{\partial \vartheta}{\partial \xi} \right] + \frac{1}{\xi} \left(1 + \frac{\Lambda}{\lambda} \right) \frac{\partial \vartheta}{\partial \xi} + \text{Pr Re}_* \text{Ec}(\varphi + \psi), \quad (11b)$$

where $\text{Pr} = \eta c_p / \lambda$ is the Prandtl number and $\text{Ec} = v_*^2 / (c_p T_0)$ is the Eckert number.

The ratio of the turbulent and molecular heat conductivity factors Λ and λ is given as:

$$\frac{\Lambda}{\lambda} = \frac{c_p \kappa_* \Theta}{\lambda \kappa \Omega} = \text{Pr Re}_* \frac{\kappa_* H}{\kappa} \left| \frac{d\xi}{dV} \right| = \text{Pr} \frac{\kappa_*}{\kappa} \frac{H}{|H - \xi|}$$

The partial differential equation (11b) can be solved for the given initial and boundary conditions when $V(\xi)$ and $H(\xi)$ are known. The similarity numbers Pr , Re_* , Ec and

$\frac{\Lambda}{\lambda}$ depend on temperature T . An approximate solution of differential equation (11b) will be proposed in the following.

2. VARIATIONAL EQUATION OF THERMAL CONVECTION-DIFFUSION PROBLEMS

It should be emphasized that the variational discussion of the convection-diffusion heat transfer problem of turbulent flow and then its p-version finite element solution constitute a new contribution part of this work.

At the given average pipe velocity v_a , the value $\tilde{\text{Ec}} = \nu_a^2/(c_p T_0)$ can be determined by interpolating c_p in Table 1 for a given temperature. According to equation (10), Re_* can be calculated, and using equation $\text{Re}_* = v_* R_0/v$, v_* will be known. Hence $\text{Ec} = v_*^2/(c_p T_0)$ and also $\text{Ec} = \tilde{\text{Ec}}/(v_a v_*)^2$ can be written.

Let us introduce the following value: $C = 1 + \frac{\Lambda}{\lambda}$.

Rewrite equation (11b) for coordinates x_1, x_2 :

$$\begin{aligned} \text{Pr Re}_* V(\xi) \frac{\partial T}{\partial x_1} \frac{R_0}{T_0} &= \frac{1}{\lambda} \left[\frac{\partial \lambda}{\partial x_1} C \frac{\partial T}{\partial x_1} \right] \frac{R_0^2}{T_0} + \frac{1}{\lambda} \left[\frac{\partial \lambda}{\partial x_2} C \frac{\partial T}{\partial x_2} \right] \frac{R_0^2}{T_0} + \\ &+ \frac{R_0^2}{T_0} \frac{\partial}{\partial x_1} \left[C \frac{\partial T}{\partial x_1} \right] + \frac{R_0^2}{T_0} \frac{\partial}{\partial x_2} \left[C \frac{\partial T}{\partial x_2} \right] + \frac{R_0^2}{T_0 x_2} C \frac{\partial T}{\partial x_2} + \\ &+ \text{Pr Re}_* \text{Ec}(\varphi + \psi). \end{aligned} \quad (12)$$

Then performing the derivations, equation (12) takes a new form:

$$\begin{aligned} \text{Pr Re}_* V(\xi) \frac{\partial T}{\partial x_1} \frac{R_0}{T_0} &= \frac{1}{\lambda} \left[\frac{\partial \lambda}{\partial x_1} C \frac{\partial T}{\partial x_1} \right] \frac{R_0^2}{T_0} + \frac{1}{\lambda} \left[\frac{\partial \lambda}{\partial x_2} C \frac{\partial T}{\partial x_2} \right] \frac{R_0^2}{T_0} + \\ &+ \frac{R_0^2}{T_0} \left\{ \frac{\partial C}{\partial x_1} \frac{\partial T}{\partial x_1} + \frac{\partial C}{\partial x_2} \frac{\partial T}{\partial x_2} + \frac{1}{x_2} C \frac{\partial T}{\partial x_2} + C \left[\frac{\partial^2 T}{\partial x_1^2} + \frac{\partial^2 T}{\partial x_2^2} \right] \right\} + \\ &+ \text{Pr Re}_* \text{Ec}(\varphi + \psi). \end{aligned} \quad (13)$$

Using the Laplace differential operator for the axisymmetric case, the following is obtained:

$$\begin{aligned} \text{Pr Re}_* V(\xi) \frac{\partial T}{\partial x_1} \frac{R_0}{T_0} &= \frac{1}{\lambda} \left[\frac{\partial \lambda}{\partial x_1} C \frac{\partial T}{\partial x_1} \right] \frac{R_0^2}{T_0} + \frac{1}{\lambda} \left[\frac{\partial \lambda}{\partial x_2} C \frac{\partial T}{\partial x_2} \right] \frac{R_0^2}{T_0} + \\ &+ \frac{R_0^2}{T_0} \left\{ \frac{\partial C}{\partial x_1} \frac{\partial T}{\partial x_1} + \frac{\partial C}{\partial x_2} \frac{\partial T}{\partial x_2} + C(\nabla^2 T) \right\} + \text{Pr Re}_* \text{Ec}(\varphi + \psi) \end{aligned} \quad (14)$$

Taking into account the definitions at the beginning of this chapter

$$\frac{\Lambda}{\lambda} = \frac{c_p \kappa_* \Theta}{\lambda \kappa \Omega} = \frac{\Lambda}{\lambda}(x_1, x_2), \quad (15)$$

this ratio depends on coordinates x_1, x_2 . Therefore the following parameter will also depend on x_1, x_2 :

$$C = 1 + \frac{\Lambda}{\lambda} = C(x_1, x_2) \quad (16)$$

Thus, differential equation (14) is written in a new form

$$\begin{aligned} \mathfrak{S} = \mathfrak{S}(T) = & \\ = & \left\{ \frac{1}{\lambda} \left[\frac{\partial \lambda}{\partial x_1} C \frac{\partial T}{\partial x_1} \right] + \frac{1}{\lambda} \left[\frac{\partial \lambda}{\partial x_2} C \frac{\partial T}{\partial x_2} \right] + \frac{\partial C}{\partial x_1} \frac{\partial T}{\partial x_1} + \frac{\partial C}{\partial x_2} \frac{\partial T}{\partial x_2} + C(\nabla^2 T) \right\} - \\ & - \text{Pr Re}_* V(\xi) \frac{\partial T}{\partial x_1} \frac{1}{R_0} + \text{Pr Re}_* \text{Ec}(\varphi + \psi) \frac{T_0}{R_0^2} \end{aligned} \quad (17)$$

or which an approximate solution is to be sought. In order to obtain a specific solution for (17) the following boundary conditions need to be prescribed.

The temperature of the inlet water on boundary Γ_1 at $x_1 = 0$ is given as

$$T = T(x_1 = 0, x_2) = T_0 \quad (18)$$

The outflow of heat flux is zero

$$\frac{\partial T}{\partial x_1} - q_{FL} = 0, \quad q_{FL} = 0 \quad \text{on boundary } \Gamma_3 \text{ at } x_1 = \infty. \quad (19a)$$

There is heat transfer on boundary Γ_2 in the cylindrical surface $x_2 = R_0$:

$$P = P(T) = \left. \frac{\partial T}{\partial x_2} \right|_{x_2=R_0} + \frac{h}{\lambda} [T(x_1, R_0) - T_K] = 0, \quad (19b)$$

where T_K is the temperature of the environment, h is the heat convection coefficient (convective heat transfer coefficient).

According to the Galerkin variation principle [12, 13] the weak form of the boundary value problem is

$$\int_{\Omega} \delta T \mathfrak{S}(T) d\Omega + \int_{\Gamma_2} \delta T P(T) d\Gamma - \int_{\Gamma_3} \delta T C \left(\frac{\partial T}{\partial x_1} - q_{FL} \right) d\Gamma = 0, \quad (20)$$

where δT is the variation of the temperature field, which is zero on the boundary Γ_1 , $\delta T = 0$.

Based on the product derivation rule

$$[\nabla \delta T \cdot C(\nabla T)] = (\nabla \delta T) \cdot C(\nabla T) + \delta T (\nabla C) \cdot (\nabla T) + \delta T C (\nabla^2 T). \quad (21)$$

Using the Gauss theorem

$$\int_{\Omega} \delta T C (\nabla^2 T) d\Omega = \int_{\Gamma_2 + \Gamma_3} \delta T C (\nabla T) \cdot \mathbf{n} d\Gamma - \int_{\Omega} \{ (\nabla \delta T) \cdot C(\nabla T) + \delta T (\nabla C) \cdot (\nabla T) \} d\Omega. \quad (22)$$

For boundary value problems (17)-(19), the Galerkin principle takes the following form:

$$\begin{aligned} \int_{\Omega} \delta T \left\{ \frac{1}{\lambda} \left[\frac{\partial \lambda}{\partial x_1} C \frac{\partial T}{\partial x_1} \right] + \frac{1}{\lambda} \left[\frac{\partial \lambda}{\partial x_2} C \frac{\partial T}{\partial x_2} \right] + \frac{\partial C}{\partial x_1} \frac{\partial T}{\partial x_1} + \frac{\partial C}{\partial x_2} \frac{\partial T}{\partial x_2} + C(\nabla^2 T) - \right. \\ \left. - \text{Pr Re}_* V(\xi) \frac{\partial T}{\partial x_1} \frac{1}{R_0} + \text{Pr Re}_* \text{Ec}(\varphi + \psi) \frac{T_0}{R_0^2} \right\} d\Omega + \\ + \int_{\Gamma_2} \delta T \left[\frac{\partial T}{\partial x_2} + \frac{h}{\lambda} (T - T_K) \right] d\Gamma - \int_{\Gamma_3} \delta T C \left(\frac{\partial T}{\partial x_1} - q_{FL} \right) d\Gamma = 0. \end{aligned} \quad (23)$$

Substituting (22) into (23) and using the following relation

$$\delta T(\nabla C) \cdot (\nabla T) = \delta T \left[\frac{\partial C}{\partial x_1} \frac{\partial T}{\partial x_1} + \frac{\partial C}{\partial x_2} \frac{\partial T}{\partial x_2} \right] \quad (24)$$

after some manipulations the final variational equation is

$$\begin{aligned} & \int_{\Omega} \left\{ -\frac{\delta T}{\lambda} \left[\frac{\partial \lambda}{\partial x_1} C \frac{\partial T}{\partial x_1} \right] - \frac{\delta T}{\lambda} \left[\frac{\partial \lambda}{\partial x_2} C \frac{\partial T}{\partial x_2} \right] + (\nabla \delta T) C \cdot (\nabla T) + \right. \\ & \left. + \delta T \text{Pr Re}_* V(\xi) \frac{\partial T}{\partial x_1} \frac{1}{R_0} \right\} d\Omega - \int_{\Gamma_2} \delta T (1 + C) \frac{\partial T}{\partial x_2} d\Gamma - \int_{\Gamma_2} \delta T \frac{h}{\lambda} T d\Gamma = \\ & = \int_{\Omega} \delta T \text{Pr Re}_* \text{Ec}(\varphi + \psi) \frac{T_0}{R_0^2} d\Omega - \int_{\Gamma_2} \delta T \frac{h}{\lambda} T_K d\Gamma + \int_{\Gamma_3} \delta T C q_{FL} d\Gamma. \end{aligned} \quad (25)$$

3. APPROXIMATION BY FINITE ELEMENT METHOD

According to the finite element method [14, 15], the temperature field is approximated in the following form:

$$T = \mathbf{N}\mathbf{q}, \quad \frac{\partial T}{\partial x_1} = \mathbf{N}_{,x1}\mathbf{q}, \quad \frac{\partial T}{\partial x_2} = \mathbf{N}_{,x2}\mathbf{q}. \quad (26)$$

Here \mathbf{N} is the matrix of shape functions, its derivatives are:

$$\frac{\partial}{\partial x_1} \mathbf{N} = \mathbf{N}_{,x1}, \quad \frac{\partial}{\partial x_2} \mathbf{N} = \mathbf{N}_{,x2}$$

and \mathbf{q} is the vector of the unknown parameters. Hierarchical shape functions will be used in p-version finite elements [14].

In order to discretize functional (25) the following formulae should be evaluated:

$$\nabla T = \begin{bmatrix} \frac{\partial \mathbf{N}}{\partial x_1} \\ \frac{\partial \mathbf{N}}{\partial x_2} \end{bmatrix} = \begin{bmatrix} \mathbf{N}_{,x1} \\ \mathbf{N}_{,x2} \end{bmatrix} \mathbf{q}, \quad (27)$$

$$\nabla T \cdot \mathbf{n} = \frac{\partial T}{\partial x_1} n_{x1} + \frac{\partial T}{\partial x_2} n_{x2} = \left[\frac{\partial \mathbf{N}}{\partial x_1} n_{x1} + \frac{\partial \mathbf{N}}{\partial x_2} n_{x2} \right] \mathbf{q} = \mathbf{\Gamma}\mathbf{q}, \quad (28)$$

$$\begin{aligned} \delta \mathbf{q}^T \mathbf{K}\mathbf{q} = & \delta \mathbf{q}^T \left(\int_{\Omega} \left\{ [\mathbf{N}_{,x1}^T \mathbf{N}_{,x2}^T] C \begin{bmatrix} \mathbf{N}_{,x1} \\ \mathbf{N}_{,x2} \end{bmatrix} + \text{Pr Re}_* [\mathbf{N}^T V \mathbf{N}_{,x1}] \frac{1}{R_0} \right\} d\Omega - \right. \\ & - \int_{\Omega} \mathbf{N}^T \frac{C}{\lambda} \left[\frac{\partial \lambda}{\partial x_1} \mathbf{N}_{,x1} + \frac{\partial \lambda}{\partial x_2} \mathbf{N}_{,x2} \right] d\Omega - \\ & \left. - \int_{\Gamma_2} \mathbf{N}^T \left[(1 + C) \mathbf{N}_{,x2} + \frac{h}{\lambda} \mathbf{N} \right] d\Gamma \right) \mathbf{q}, \end{aligned} \quad (29)$$

$$\delta \mathbf{q}^T \mathbf{f} = \delta \mathbf{q}^T \left(\frac{T_0}{R_0^2} \int_{\Omega} \mathbf{N}^T \text{Pr Re}_* \text{Ec}(\varphi + \psi) d\Omega - \int_{\Gamma_2} \mathbf{N}^T \frac{h}{\lambda} T_K d\Gamma + \int_{\Gamma_3} \mathbf{N}^T C q_{FL} d\Gamma \right). \quad (30)$$

The stiffness matrix \mathbf{K} and the load vector \mathbf{f} are produced by Gauss type numerical integration element by element. In order to evaluate the above expressions the fluid flow problem should be solved first, and accordingly the values of V , C , φ and ψ at these points are taken. The rest of the parameters are interpolated from Table 1, the Reynolds numbers can be taken from Figures 25 and 26 as a function of the fluid rate.

Due to arbitrary variation of $\delta\mathbf{q}$, the following algebraic equation system needs to be solved:

$$\mathbf{K}\mathbf{q} - \mathbf{f} = \mathbf{0}. \tag{31}$$

Its solution is given as

$$\mathbf{q} = \mathbf{K}^{-1}\mathbf{f}. \tag{32}$$

The temperature field is approximated by (26), the material constants are modified accordingly, then by the repeatedly calculated stiffness matrix \mathbf{K} and load vector \mathbf{f} , equation (26) will be solved successively until the following tolerance has been met as far as the following inequality:

$$e_T = 100 \frac{\sqrt{\sum_i (q_i^{(s)})^2} - \sqrt{\sum_i (q_i^{(s-1)})^2}}{\sqrt{\sum_i (q_i^{(s-1)})^2}} \leq 0.001, \tag{33}$$

where s is the number of iteration.

4. NUMERICAL RESULTS

Let us examine the flow of water in a rigid pipe. The temperature is given at the inlet edge of the pipe. Our aim is to determine the frictional heat generation caused by the turbulent flow, which will affect the water temperature. The following questions can also be examined: How will the temperature change with different heat transfer parameters, and how will the volume flow rate Q affect the resulting temperature field? It is also a question whether the solution is sensitive to the diameter of the pipe, i.e., whether it is significant or not.

Let the reference temperature and the environment temperature be $T_0 = 373$ K and $T_K = 293$ K, respectively.

Material constants are independent of fluid velocity but depend on the temperature in the case of water as given in Table 1.

Table 1.

$T [^\circ\text{C}]$	0	20	100
$\rho [\text{kg}/\text{m}^3]$	1002.28	1000.52	960.63
$c_p [J/(\text{kgK})]$	4118	4182	4216
$\nu = \eta/\rho [\text{m}^2/\text{s}]$	1.788×10^{-6}	1.116×10^{-6}	2.94×10^{-7}
$\lambda [W/(\text{mK})]$	0.552	0.597	0.680
Pr	13.369	7.821	1.751

In the solution process, first the functions $V(\xi)$ and $H(\xi)$ are determined by solving the fluid flow problem. The viscous and turbulent dissipations depend on these functions:

$$\varphi = \frac{R_0 \varphi_D}{v_*^3} = \frac{1}{\text{Re}_*} \left(\frac{dV}{d\xi} \right)^2, \quad \psi = \frac{R_0 \varepsilon}{v_*^3} = -\frac{\alpha + 2\beta + \gamma}{4 \text{Re}_* H} \left(\frac{dH}{d\xi} \right)^2. \quad (34)$$

Dissipation leads to an increase in the temperature of the fluid. Two cases will be demonstrated here. Let us take two different pipe diameters (D) with the same flow rate Q . The results are shown in Figure 2.

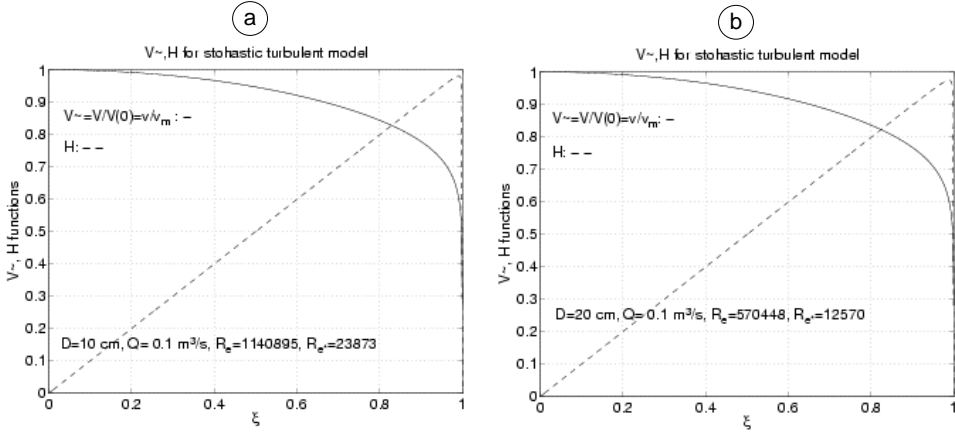


Figure 2. Functions V^- and H^- along the radius, a) $D = 0.1\text{m}$,
b) $D = 0.2\text{ m}$

It can be seen that around the pipe wall ($x_2 \sim R_0$, $\xi \sim 1$), both functions change abruptly, since the heat development is significant there.

Let us consider the pressure distribution. The following equations for the pressure can be obtained by integrating differential equation (5a) using transformation $H(\xi) = \Theta/(\rho v_*^2)$ in it.

$$p^{\sim}(\xi) - p_0 = \frac{p(\xi)}{\rho v_*^2} - \frac{p_0}{\rho v_*^2} = \left(\beta_* - \frac{2a^2}{3} \right) H + (\beta_* - \gamma_*) \int_0^\xi \frac{1}{\xi} H d\xi \quad (35a)$$

$$p(x_1, x_2) = A(x_2) + Bx_1 = p^{\sim}\left(\frac{x_2}{R_0}\right) - \frac{\Delta p}{L} x_1. \quad (35b)$$

From Figure 26 at $Q = 0.1\text{ m}^3/\text{s}$, $v_a = 3.1831\text{ m/s}$, Reynolds numbers are $\text{Re} = 570448$, $\text{Re}_* = 12680$ and taking $D = 0.2\text{ m}$, it follows that

$$v_* = \frac{\text{Re}_* v}{R} = \frac{12680 \times 1.116}{10^5} = 0.1415\text{ m/s}.$$

Furthermore

$$\rho v_*^2 = 1000.52 \times 0.1415^2 = 20.03 \frac{\text{kg}}{\text{ms}^2} = 20.03\text{ Pa} = 20.03 \times 10^{-5}\text{ bar}.$$

Pressure p^{\sim} changes as shown in Figure 3a at $p^{\sim} = 1$. If $p_0 > \rho v_*^2$ then the point ($\xi = 0$, $p^{\sim}(0) = 1$) shifts to a vertically higher position, and the function $p^{\sim}(\xi)$ will be parallel to the current situation.

Computations are repeated for pipes of $D = 0.1\text{m}$ and $D = 0.3\text{m}$, obtaining the pressure distributions are shown in Figure 3b. For all the three different pipe diameters, the pressures are similar and they increase slightly at the vicinity of the wall. The larger the pipe diameter, the greater the rate of change $\Delta p^{\sim} = 1 - p^{\sim}(\xi = 1)$. The maximum rate of change of pressure with respect to its maximum value is $\sim 0.8(\rho v_*^2)$.

When the friction factor f for the pipe is known, the pressure loss can be calculated as follows [16]:

$$\Delta p = f \frac{L}{D} \frac{\rho}{2} v_a^2 = 8f \frac{L}{D^5 \pi^2} \rho Q^2 \quad [\text{Pa}]. \quad (36)$$

Taking a pipe of $D = 0.2\text{m}$ and $f = 0.02$, the pressure drop for one meter length is

$$\Delta p = 8f \frac{L}{D^5 \pi^2} \rho Q^2 \quad [\text{Pa}] = 8 \times 0.02 \frac{1}{0.2^5 \pi^2} 1000.52 \times 0.1^2 = 506.87 \text{ Pa} = 0.0050687 \text{ bar}.$$

This means that the pressure drops are 5.068 bar for length L of 1 km, 25.34 bar for 5 km and 50.68 bar for 10 km, resp.

The supply pressure is determined by the pressure drop along the pipe. For smaller diameters, its value increases significantly, which will affect the performance of the pump used.

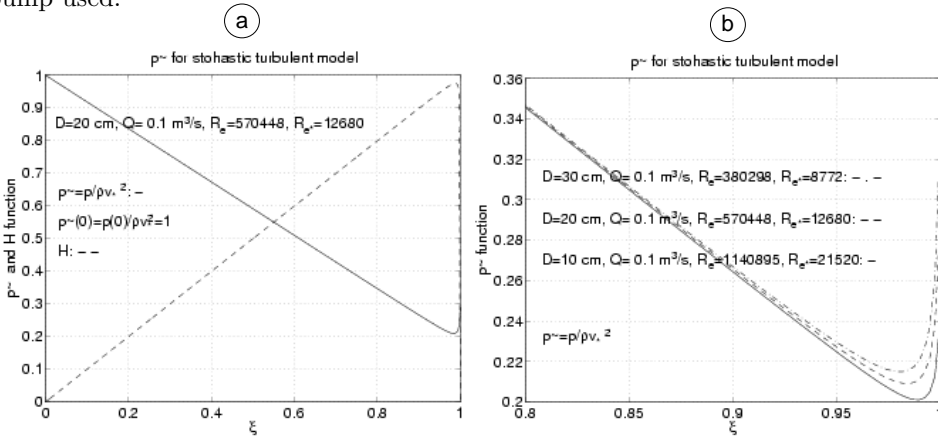


Figure 3. $p^{\sim}(\xi)$ pressure at $p^{\sim}(0) = 1$, a) along the radius, b) in the vicinity of the pipe wall

4.1. Examination of a five kilometer long pipe. If the diameter of the pipe is $D = 0.2\text{m}$ and its length is 5 km, the corresponding finite element mesh is indicated in the figures for temperature. Thin lines that appear for each element correspond to coordinate lines passing through Gaussian (Lobatto) numerical integration points. The polynomial order of each element is $p = 8$. The elements applied are ring elements, which are suitable for describing axially symmetrical relationships. Small elements were taken to better approximate the flow in the boundary layer

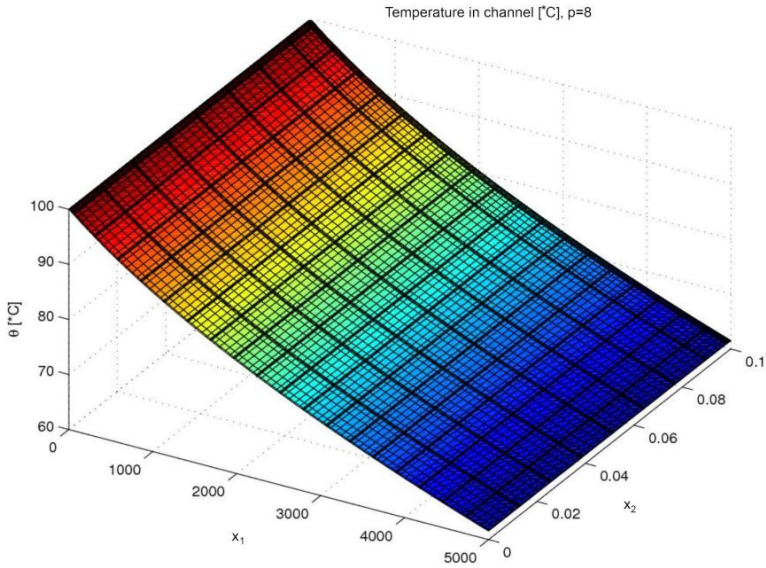


Figure 4. Resulting temperature distribution at $R_0 = 0.1$ m, $Q = 0.009$ m³, $h = 7.71$ W/(m²K)

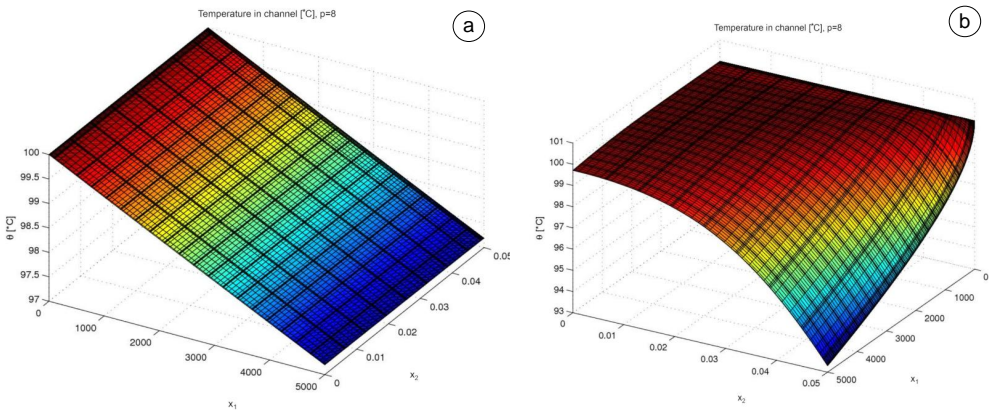


Figure 5. Resulting temperature for parameters $Q = 0.03$ m³/s, $h = 2.22$ W/(m²K), a) in case of turbulent flow (with heat generation), b) without heat generation for diameter $D = 0.1$ m

near the edge $x_2 = R_0$. The same dense mesh is applied in the direction of the longitudinal axis at the entry cross-section.

Figures 25 and 26 show flows of fluids Q [m³/s], with average velocity v_a [m/s], and the Reynolds number Re depending on the radius R_0 of the pipe and the Re_* number.

Temperature changes are computed for two different convective heat transfer coefficients h [W/(m²K)] and for parameters $R_0 = 0.1$ m, $Q = 0.009$ m³/s, $h = 7.71$ W/(m²K), shown in Figure 5. In Figure 6 the temperature of the fluid is shown in turbulent flow under parameters: $R_0 = 0.1$ m, $Q = 0.04$ m³/s, $h = 2.22$ W/(m²K) with and without frictional heat generation. The length of the pipe is 5000 m. In all figures temperature T is denoted by θ .

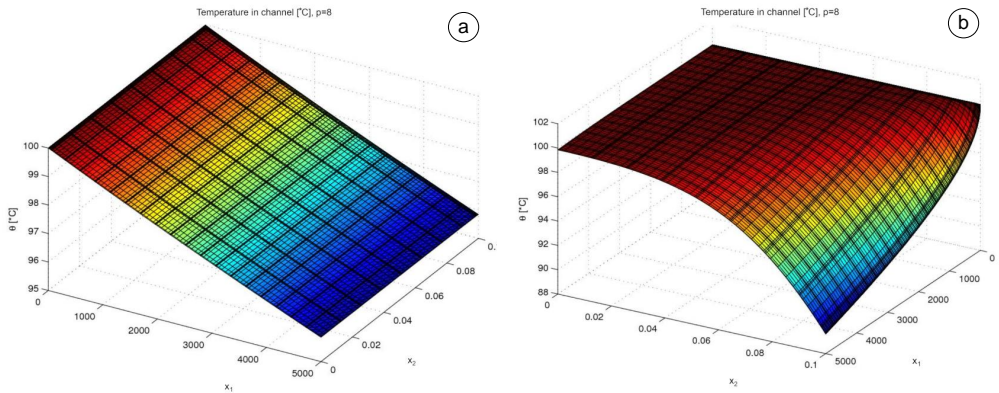


Figure 6. Resulting temperature for parameters $Q = 0.04$ m³/s, $h = 2.22$ W/(m²K), a) in case of turbulent flow (with heat generation), b) without heat generation for diameter $D = 0.2$ m

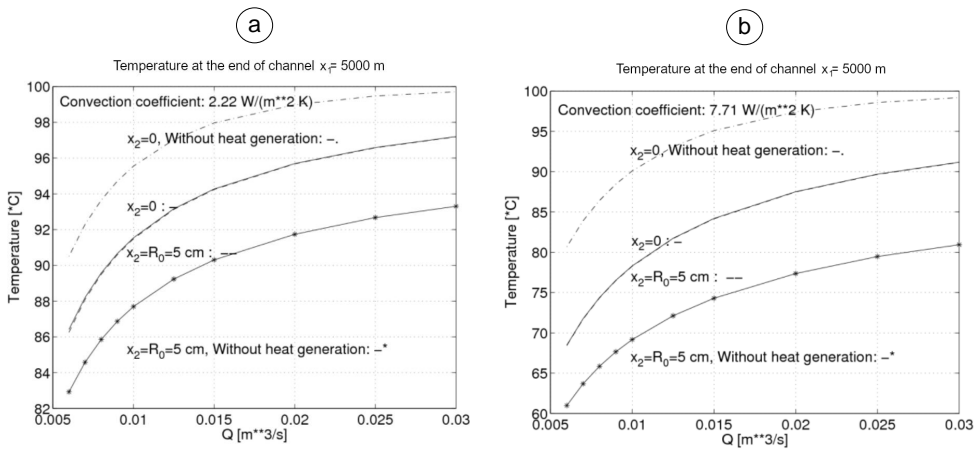


Figure 7. Temperature distributions in the case of pipe radius $R_0 = 0.05$ m, as a function of volume current Q (-,-) with and without heat generation (-*,-); a) $h = 2.22$ W/(m²K), b) $h = 7.71$ W/(m²K)

It is very clear that in computations without heat generation, the temperature changes along the radius of the pipe are significant, and the heat losses along the length are much greater than in cases of frictional internal heat generation resulting

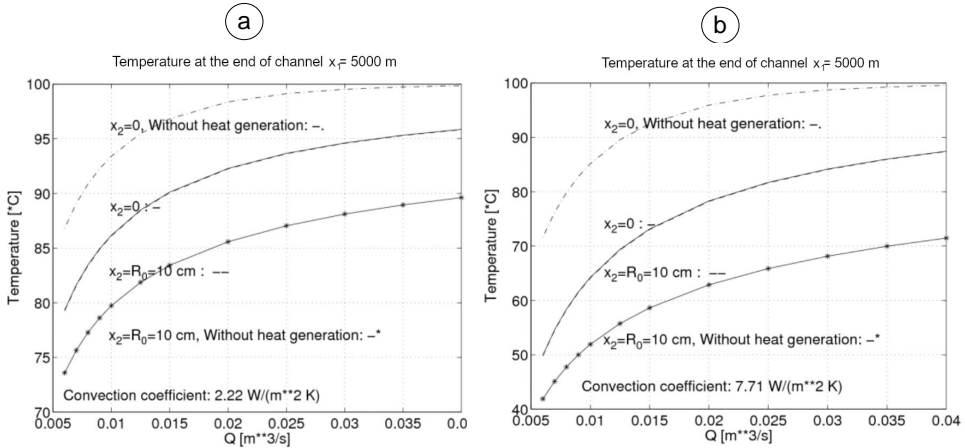


Figure 8. Temperature distributions in the case of pipe radius $R_0 = 0.01$ m, as a function of volume current Q (-,-) with heat generation, and for cases without heat generation (-*,-); a) $h = 2.22$ W/(m²K), b) $h = 7.71$ W/(m²K)

from the turbulence. Therefore, turbulence reduces the cooling of the water flowing in the pipe; the higher the Reynolds number, the smaller the heat loss. It can also be seen that the value of the heat transfer factor significantly affects the temperature that develops. The high-efficiency thermal insulation of the pipe is very important in order to provide the water temperature at the end of the transmission line that is desired for heating.

Summarizing the computational results, in Figures 7 and 8, at the center of the pipe $x_2 = 0$, and at the outer radius of the pipe $x_2 = R_0$ curves are denoted with (-) continuous, (-) dashed curves for turbulent flow, resp., while curves (-*) and (-.) are associated with the case without heat generation. The temperatures are evaluated at the cross-section points at the end of a pipe section $x_1 = 5000$ m. The higher the flow rate Q , the less water will cool along the length of the pipe.

4.2. Analyses of pipes with lengths of ten and fifteen kilometers without heat generation.

4.2.1. Temperature in a ten kilometer long pipe:

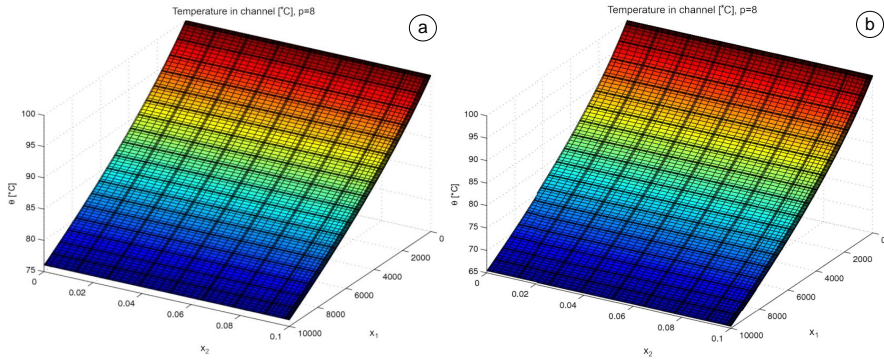


Figure 9. Temperature that develops for a) $Q = 0.01 \text{ m}^3$, b) $Q = 0.006 \text{ m}^3$ at $D = 0.2 \text{ m}$ if $h = 2.22 \text{ W}/(\text{m}^2\text{K})$, $L = 10 \text{ km}$

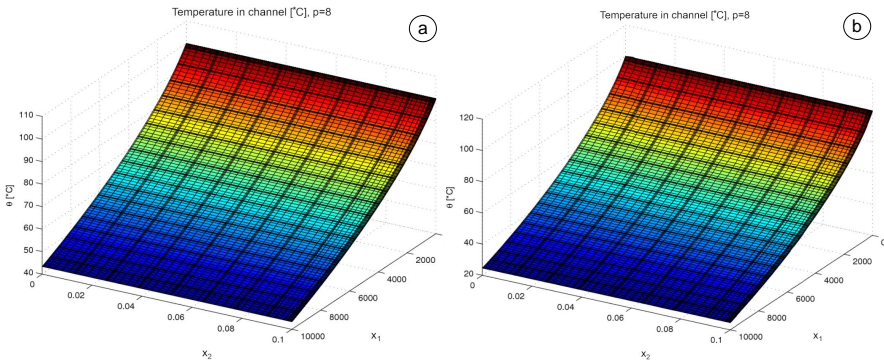


Figure 10. Temperature that develops for a) $Q = 0.01 \text{ m}^3$, b) $Q = 0.006 \text{ m}^3$ at $D = 0.2 \text{ m}$ if $h = 7.71 \text{ W}/(\text{m}^2\text{K})$, $L = 10 \text{ km}$

4.2.2. Temperature in a fifteen kilometer long pipe:

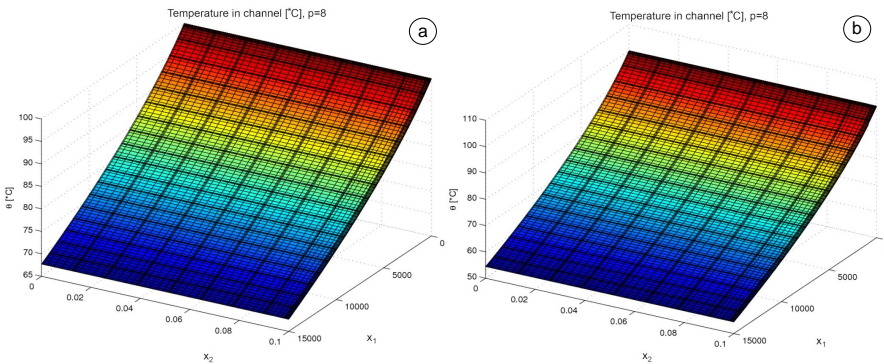


Figure 11. Temperature that develop for a) $Q = 0.01 \text{ m}^3$, b) $Q = 0.006 \text{ m}^3$ at $D = 0.2 \text{ m}$ if $h = 2.22 \text{ W}/(\text{m}^2\text{K})$, $L = 15 \text{ km}$

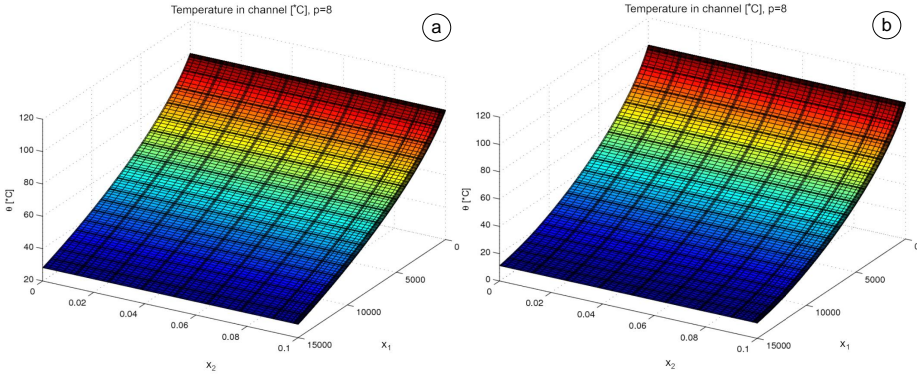


Figure 12. Temperature that develops for a) $Q = 0.01 \text{ m}^3$, b) $Q = 0.006 \text{ m}^3$ at $D = 0.2 \text{ m}$ if $h = 7.71 \text{ W}/(\text{m}^2\text{K})$, $L = 15 \text{ km}$

4.2.3. Temperature in a twenty kilometer long pipe:

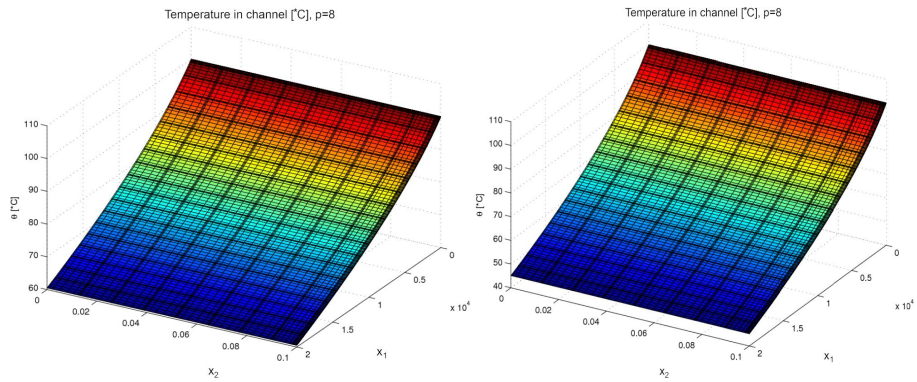


Figure 13. Temperature that develops for a) $Q = 0.01 \text{ m}^3$, b) $Q = 0.006 \text{ m}^3$ at $D = 0.2 \text{ m}$ if $h = 2.22 \text{ W}/(\text{m}^2\text{K})$, $L = 20 \text{ km}$

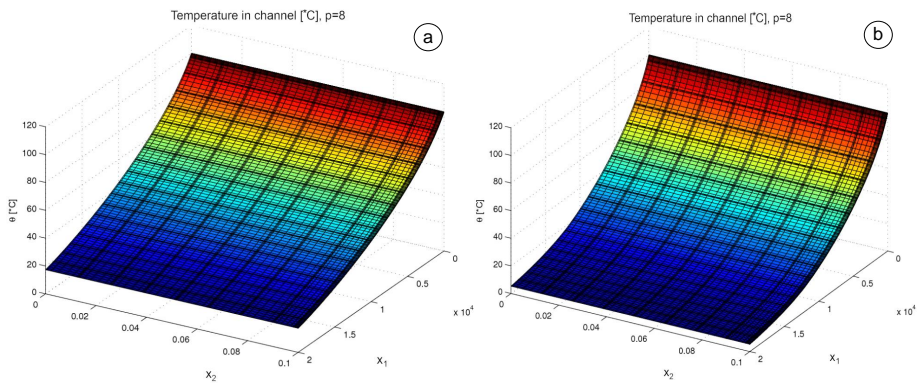


Figure 14. Temperature that develops for a) $Q = 0.01 \text{ m}^3$, b) $Q = 0.006 \text{ m}^3$ at $D = 0.2 \text{ m}$ if $h = 7.71 \text{ W}/(\text{m}^2\text{K})$, $L = 20 \text{ km}$

Figures 9-14 show the temperature distributions obtained in some of the numerous cases examined.

Figure 15 shows the temperature for pipe diameter $D = 0.1$ m for different heat transfer factors. Figure 16 demonstrates that for a low-value of volume flow rate Q heat loss is very significant, especially for larger $h = 7.71$ W/(m²K). For $Q = 0.006$ m³, the water has practically taken on the temperature of the environment already at $x_1 = 10$ km distance.

For the larger diameter $D = 0.2$ m the results are more favorable as regards the cooling process (see Figure 16), but the cooling of the water will be significant for a small value of Q . Here the case without heat generation is also indicated. The effect of heat generation is noticeable. For example with $Q = 0.035$ m³/s, the temperature is about 7 °C higher at the output cross-section of the pipe than for a non-heat generation assumption (see Figure 16a, b). The same can also be seen for $Q = 0.1$ m³/s (see Figure 16c, d).

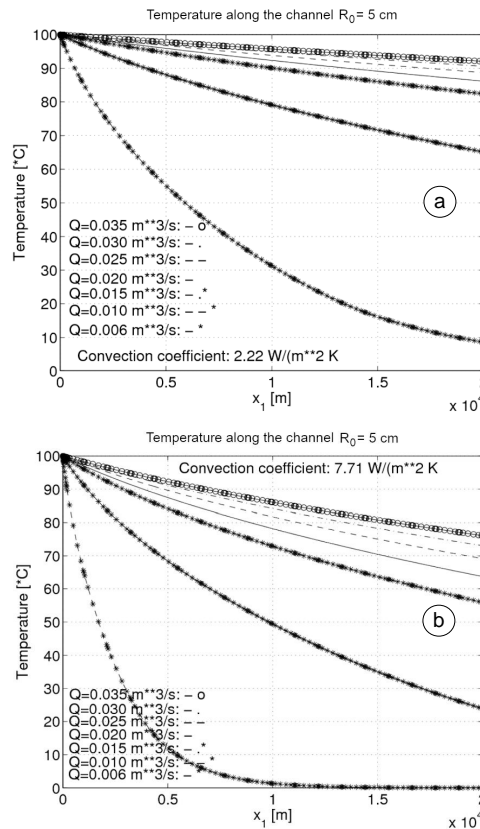


Figure 15. Temperature distribution at the edge of a pipe ($x_2 = R_0$) for different Q values if diameter is $D = 0.1$ m and the pipe length is $L = 20$ km, and there is no heat generation, a) $h = 2.22$ W/(m²K), b) $h = 7.71$ W/(m²K)

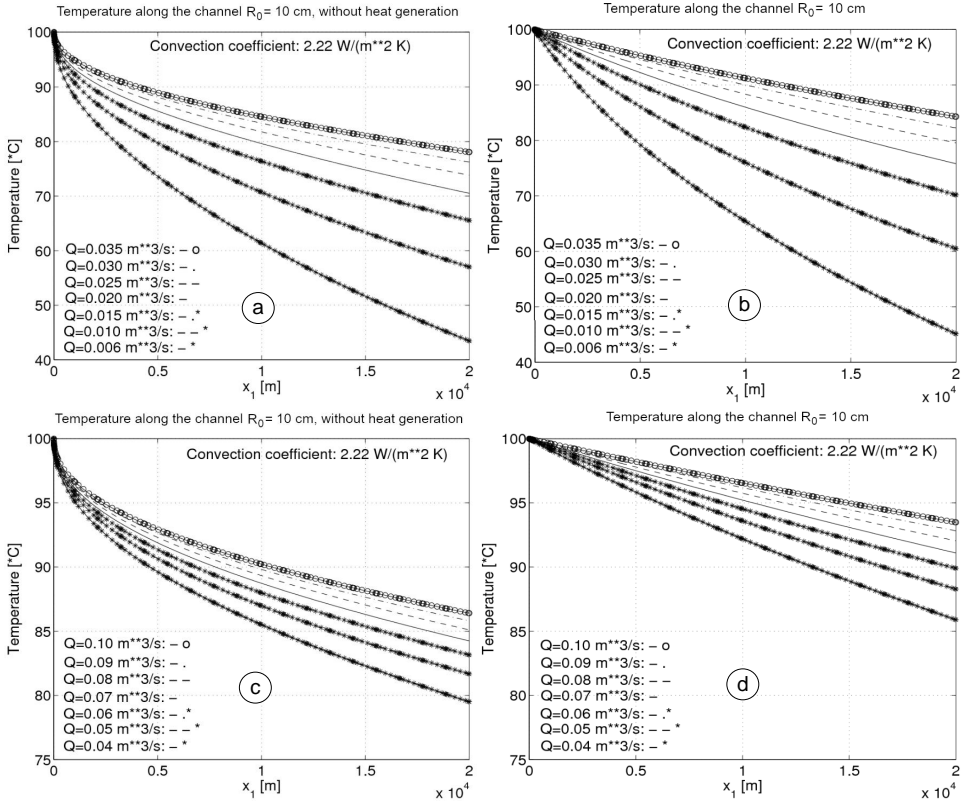


Figure 16. Temperature distribution at the edge of a pipe ($x_2 = R_0$) for different Q values if $D = 0.2$ m, $L = 20$ km; a) and c) without heat generation b) and d) with heat generation

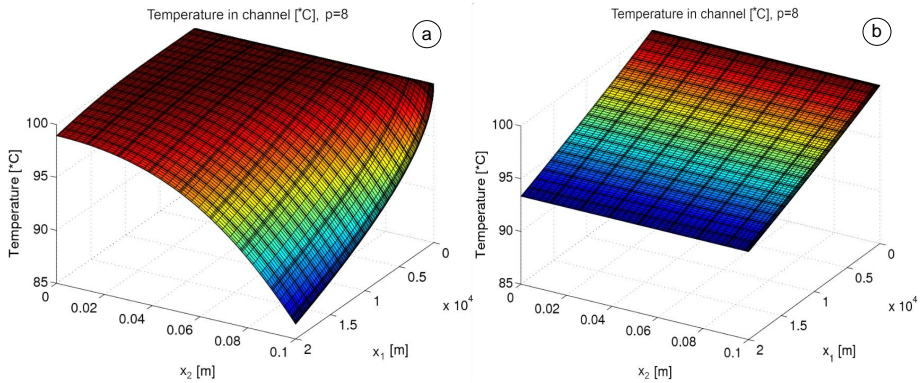


Figure 17. Temperature that develops for $Q = 0.1$ m³ at $D = 0.2$ m if $h = 2.22$ W/(m²K); a) without heat generation b) with heat generation

Figure 17 shows the temperature distribution for values of $Q = 0.1 \text{ m}^3$ and $h = 2.22 \text{ W}/(\text{m}^2\text{K})$. The results obtained for higher $h = 7.71 \text{ W}/(\text{m}^2\text{K})$ are shown in Figure 19.

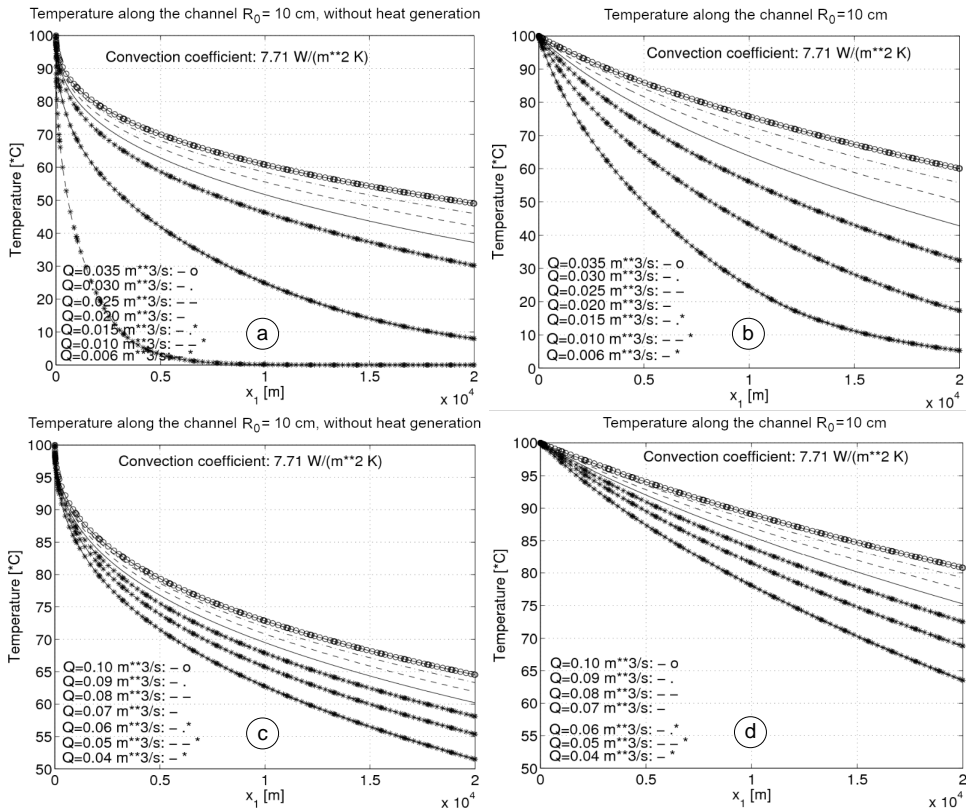


Figure 18. Temperature distribution at the edge of a pipe ($x_2 = R_0$) for different Q values if $D = 0.2 \text{ m}$, $L = 20 \text{ km}$; a)c) without heat generation b)d) with heat generation

As noted above, the higher the velocity of the water, the less it cools down. Figure 19 shows the temperature distribution for values of $Q = 0.1 \text{ m}^3$ and $h = 7.71 \text{ W}/(\text{m}^2\text{K})$.

We can get an illustrative picture of how the final cross-sectional pipe wall temperature changes as a function of the parameters Q and v_a depending on the two heat transfer factors $h = 2.22 \text{ W}/(\text{m}^2\text{K})$ and $h = 7.71 \text{ W}/(\text{m}^2\text{K})$ (see Figure 20). For $h = 7.71 \text{ W}/(\text{m}^2\text{K})$, the pipe wall temperature changes will be small above certain values of Q or v_a .

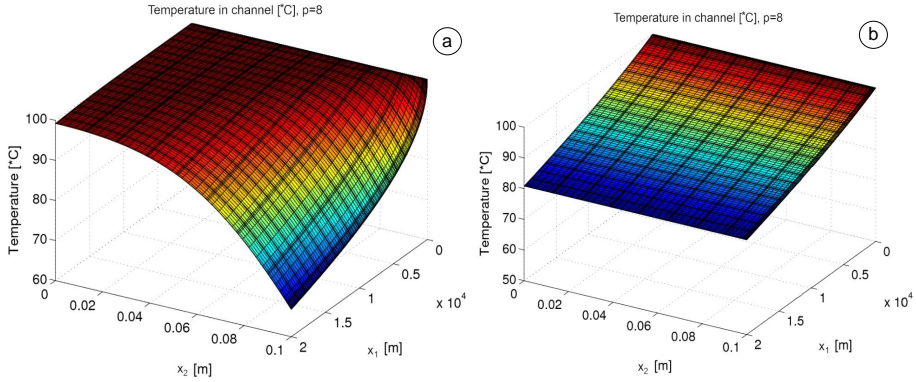


Figure 19. The resulting temperature for parameters $Q = 0.1 \text{ m}^3$, $h = 7.71 \text{ W}/(\text{m}^2\text{K})$; at $D = 0.2 \text{ m}$ a) without heat generation b) with heat generation

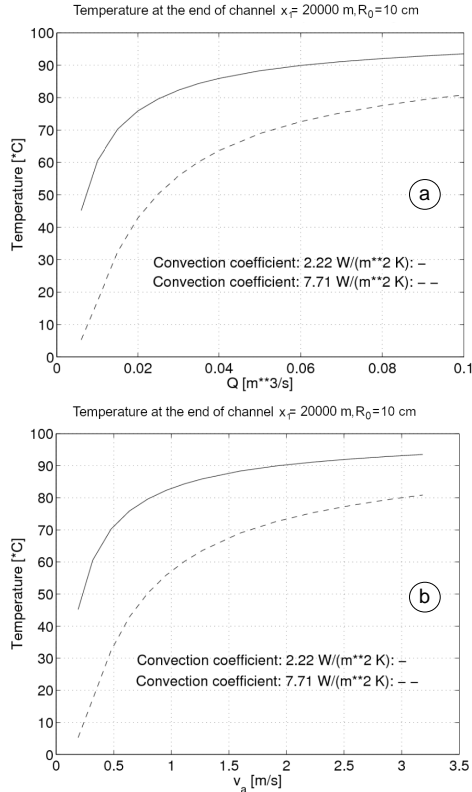


Figure 20. The resulting temperature at the boundary ($x_2 = R_0$) of the cross section $x_1 = 20 \text{ km}$ for parameters $h = 2.22 \text{ W}/(\text{m}^2\text{K})$, $h = 7.71 \text{ W}/(\text{m}^2\text{K})$, $D = 0.2 \text{ m}$ a) as a function of Q b) as a function of v_a [m/a]

Finally, performing the computations for a pipe with a diameter of $D = 0.3$ m, the results are shown in Figures 21-24.

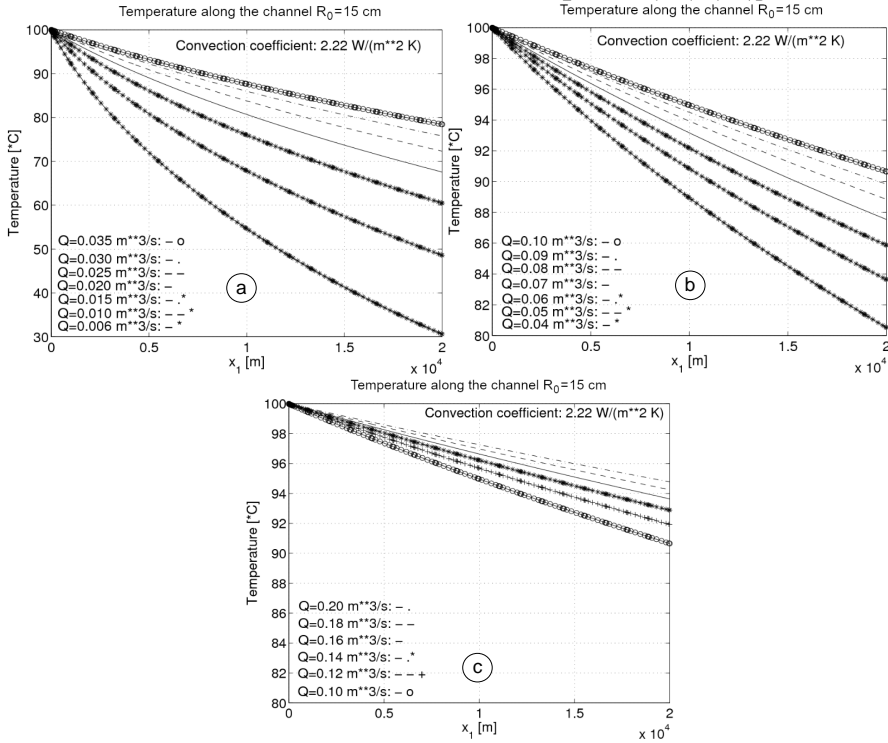


Figure 21. Temperature distribution at the edge of a pipe with turbulent flow for different Q values for diameter $D = 0.3$ m and pipe length $L = 20$ km; $h = 2.22$ W/(m²K) with heat generation taken into account

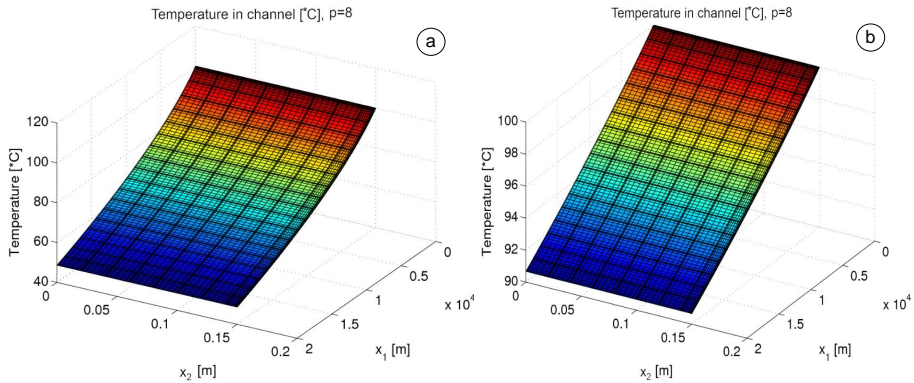


Figure 22. Temperature distribution obtained with heat generation for turbulent flow for parameter $h = 2.22$ W/(m²K), in the case of diameter $D = 0.3$ m; a) $Q = 0.01$ m³, b) $Q = 0.1$ m³

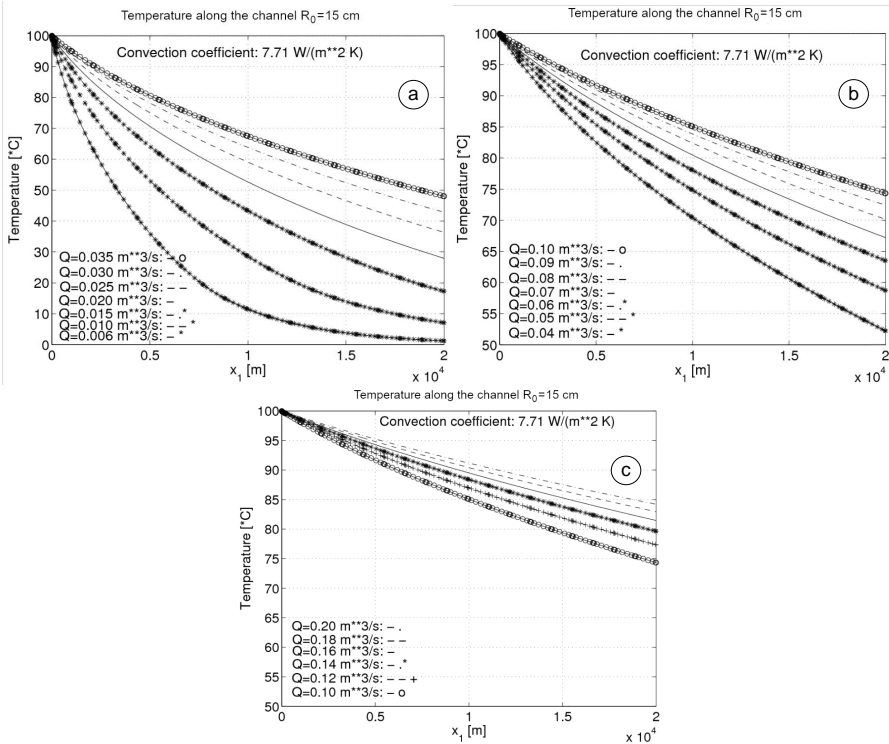


Figure 23. Temperature distribution at the edge of a pipe with turbulent flow for different Q values for diameter $D = 0.3$ m and pipe length $L = 20$ km ; $h = 7.71$ W/(m²K) with heat generation taken into account

4.3. **Comparison.** The computed temperature results obtained for the same flow rate $Q = 0.1$ m³/s but for different pipe diameters D are given in Table 2. Comparing the temperatures for different diameters the following can be stated: the greater the diameter, the higher the temperature drop for different values of h .

Table 2.

	D [cm]	$T(x_1 = 10)$ km	$T(x_1 = 20)$ km
$h = 2.22$ W/(m ² K)	$D = 20$ [cm]	96.5	93
	$D = 30$ [cm]	95	91
$h = 7.71$ W/(m ² K)	$D = 20$ [cm]	89	82
	$D = 30$ [cm]	85	74

The longer the pipe, the lower the temperature of the fluid at the end of the tube, and the slower the flow rate (i.e., Q is small), the greater the loss due to the heat transfer between the pipe and the environment. In this case, the fluid cools down significantly (see Figures 18b, 21a, and 23a). As Q increases, the temperature function $T(x_1, R_0)$ decreases virtually linearly along the length of the pipe. These results are consistent with practical, engineering experience.

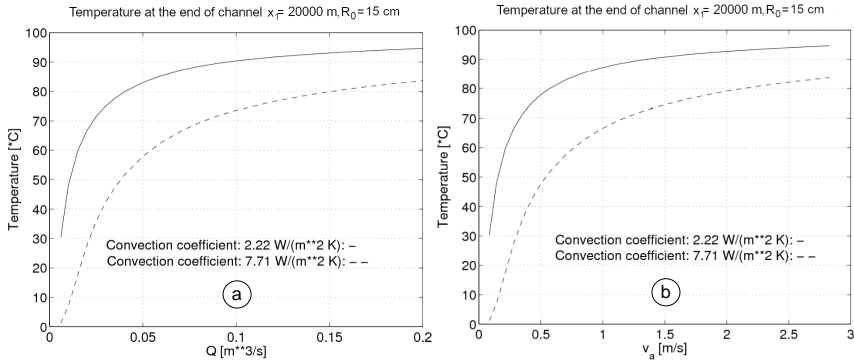


Figure 24. The resulting temperature at $x_1 = 20$ km in the boundary $x_2 = 20$ km for parameters $h, D = 0.3$ m a) depending on Q . b) depending on the average velocity v_a [m/s]

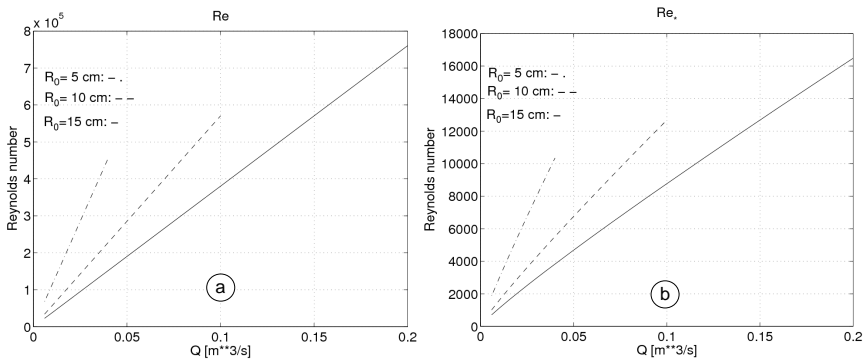


Figure 25. Functions a) for Reynolds number, b) for Re_* depending on the flow rate Q of the current for different pipe diameters

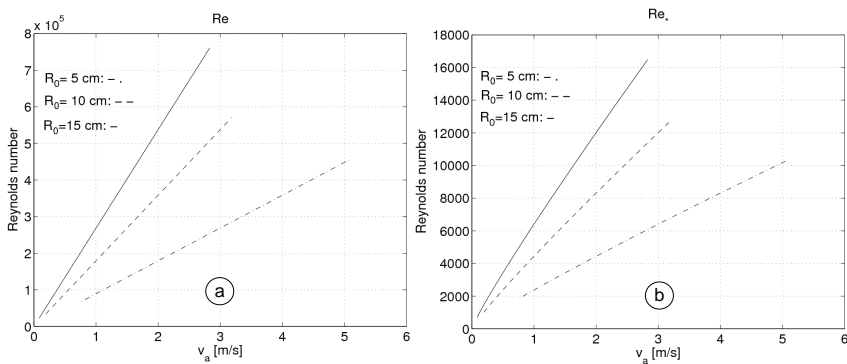


Figure 26. Functions a) for Reynolds number, b) for Re_* depending on the average velocity v_a [m/s] of the current for different pipe diameters

4.4. Reliability of the FEM computations. It is important to be aware of the error in the computations presented. A comprehensive analysis of the issue can be found in [14]. A relatively simple way to do this is to check the accuracy of the computed boundary conditions. The accuracy of the solution is expressed by the extent to which the boundary conditions are satisfied. In this aspect, the tests will be performed below. On the surface we will check the fulfillment of the boundary condition.

Let us begin with the heat transfer boundary condition on (see (19b)):

$$-\frac{\partial T}{\partial x_2} \Big|_{x_2=R_0} = \frac{h}{\lambda} [T(x_1, R_0) - T_K]. \quad (37)$$

Taking the derivative in the direction $y = R_0 - x_2$, the following equation is obtained

$$\frac{\partial T}{\partial y} \Big|_{y=0} = \frac{h}{\lambda} [T(x_1, R_0) - T_K]. \quad (38)$$

Let us define the following dimensionless quantities

$$T^* = \frac{T - T_K}{T_{y=0} - T_K}, \quad y^* = y/(2R_0). \quad (39)$$

Using them, the heat transfer coefficient can be expressed as

$$h = \frac{\lambda}{T_{y=0} - T_K} \frac{\partial T}{\partial y} \Big|_{y=0} = \lambda \frac{T_{y=0} - T_K}{T_{y=0} - T_K} \frac{1}{2R_0} \frac{\partial T^*}{\partial y^*} = \frac{\lambda}{2R_0} \frac{\partial T^*}{\partial y^*} \Big|_{y^*=0} \quad (40)$$

from which the Nusselt number can be defined [17, 18]

$$\text{Nu} = \frac{h2R_0}{\lambda} = \frac{\partial T^*}{\partial y^*} \Big|_{y^*=0}. \quad (41)$$

The derivative $\partial T^*/\partial y^*|_{y^*=0}$ can be calculated from the FEM solution, and on the other hand, its value $h2R_0/\lambda$ is easy to obtain. The difference between these values provides a piece of information about the errors of the FEM computations.

A concrete example is taken for turbulent flow without heat generation (see Temperature distribution in Figure 17a). The derivative is evaluated in the section $x_1 = 20$ km.

Using the difference method, the derivative $\partial T^*/\partial y^*|_{y^*=0} = 0.7$. The formula $h2R_0/\lambda$ can be calculated using the interpolation of λ in Table 1:

$$\lambda(80^\circ\text{C}) = 0.665 \text{ W}/(\text{m}^2\text{K}).$$

Then its value

$$\frac{h2R_0}{\lambda} = \frac{2.22 * 0.2}{0.665} = 0.667.$$

Finally, the error is

$$e_{Nu} = \frac{0.7 - 0.667}{0.667} 100\% \approx 5\%,$$

which confirms that the solution is fairly good. Similar errors are obtained for the other solutions as well.

5. CONCLUSIONS

A thermal convection-diffusion problem is investigated based on the turbulence model developed by Professor Czibere [1–3], which is solved for pipelines by the finite element approximation method in this paper. High-precision results can be obtained with the chosen p-version finite elements [12]. The program developed is well suited for flow and thermal design of pipelines. Using the computer program developed, the computations can be performed at great speed using the actual geometrical and material data. The results, i.e., radial and longitudinal distributions of temperature, are displayed graphically, which helps the designer to consider the effects of the selected diameter D of the pipe, the flow rate Q , and the heat transfer constant h in order to analyze the implementation costs of the pipeline.

Acknowledgement. The present research was partly supported by the Hungarian Academy of Sciences and the SROP-4.2.1.B-10/2 / KONV-2010-0001 program. The author would like to thank Professor Tibor Czibere for raising the research topic of the article and also for permission to use a computer program suitable for the computation of turbulent flow in a pipe. His helpful discussion of the introductory part of the paper and the computed results is also acknowledged

NOMENCLATURE

Latin notations

- c_P special heat at constant pressure [J/(kgK)]
- D diameter of the pipe
- $Ec = v_*^2 / (c_P T_0)$ Eckert number
- f friction factor
- h convective heat transfer coefficient [W/(m²K)]
- \mathbf{H} and \mathbf{H}^* similarity tensor and its deviator
- \mathbf{G} eddy viscosity tensor
- \mathbf{g} acceleration due to gravity [m/s²]
- $k = \frac{1}{2} \overline{(\mathbf{v}' \cdot \mathbf{v}')} = a^2 (\kappa l \Omega)^2 = a^2 \Theta / \rho$ turbulent kinetic energy [m²/s²]
- l length scale of turbulence [m]
- $l\Omega$ velocity scale of turbulence [m/s]
- p pressure [Pa]
- Δp pressure drop [Pa]
- $Pr = \eta c_P / \lambda$ Prandtl number
- R_0 inner radius
- Re Reynolds number
- $Re_* = v_* R_0 / \nu$ factor
- Q volume flow rate [m³/s]
- t time [s]
- T absolute temperature [K]
- T_0 reference temperature [K]
- T_K temperature of the environment [K]
- \mathbf{v} velocity vector with components v_1, v_2, v_3 [m/s]
- \mathbf{v}' velocity vector for turbulent fluctuations [m/s]

v_* wall friction velocity [m/s]

v_a average velocity [m/s]

x_1, x_2, x_3 coordinates in the computation coordinate system

Greek notations

α, β, γ parameters in \mathbf{H} similarity tensor

$$\varepsilon = v(\mathbf{v}' \circ \nabla) : (\mathbf{v}' \circ \nabla + \nabla \circ \mathbf{v}') = -v \frac{\alpha + 2\beta + \gamma}{4\rho\Theta} \left(\frac{d\Theta}{dx_2} \right)^2 \text{ turbulent dissipation [m}^2/\text{s}^2]$$

η dynamic viscosity [Pa]

$\Theta = \rho(\kappa l \Omega)^2$ dominant turbulent shear stress [Pa]

$\kappa = 0.407$ Kármán constant

$\kappa_* = 0.47$

λ thermal conductivity [W/(mK)]

$\Lambda = \rho c_P \kappa \kappa_* l^2 \Omega$ turbulent thermal conductivity [W/(mK)]

$\nu = \eta/\rho$ kinematic viscosity [m²/s²]

ρ density of the fluid [kg/m³]

$$\phi_D = v(\mathbf{v} \circ \nabla) : (\mathbf{v} \circ \nabla + \nabla \circ \mathbf{v}) = v \left(\frac{dv_1}{dx_2} \right)^2 \text{ viscous dissipation [m}^2/\text{s}^3]$$

$$\phi = \frac{R\phi_D}{v_*^3} = \frac{1}{\text{Re}_*} \left(\frac{dV}{d\xi} \right)^2 \text{ function for modified viscous dissipation [m}^2/\text{s}^3]$$

$$\psi = \frac{R\varepsilon}{v_*^3} = -\frac{\alpha + 2\beta + \gamma}{4\text{Re}_* H} \left(\frac{dH}{d\xi} \right)^2 \text{ function for modified turbulent dissipation [m}^2/\text{s}^3]$$

$\Omega = \nabla \times \mathbf{v}$ vortex vector [1/s]

$|\Omega| = \nabla \times \mathbf{v}|$ absolute value of the vortex vector [1/s]

Dimensionless quantities

$$H(\xi) = \frac{\Theta}{\rho v_*^2}$$

$$V(\xi) = \frac{v_1}{v_*}$$

$$\vartheta = \frac{T}{T_0}$$

$$\xi = \frac{x_2}{R}$$

REFERENCES

1. T. Czibere. "Three dimensional stochastic model of turbulence." *Journal of Computational and Applied Mechanics*, **2**(1), (2001), pp. 7–20. URL: <http://www.mech.uni-miskolc.hu/jcam/>.
2. T. Czibere. "Calculating turbulent flows based on a stochastic model." *Journal of Computational and Applied Mechanics*, **7**(2), (2006), pp. 155–188. URL: <http://www.mech.uni-miskolc.hu/jcam/>.

3. T. Czibere. *Transport theory solution of the turbulent flow problem based on the stochastic turbulence model*. in Hungarian. Report. University of Miskolc, Hungary, 2012. 37 pp.
4. N. Reddy and D. K. Gartling. *The Finite Element Method in Heat Transfer and Fluid Dynamics*. CRC Press, 1994. Chap. 8.2. 524 pp.
5. M. Griebel, T. Dornsheifer, and T. Neunhoeffler. *Numerical Simulation in Fluid Dynamics. A Practical Introduction*. Society for Industrial and Applied Mathematics, 1998. Chap. 10. xvi + 208. DOI: 10.1137/1.9780898719703.
6. T. J. Chung. “Applications to Turbulence.” *Computational Fluid Dynamics*. Cambridge University Press, 2002, 679–723. DOI: 10.1017/CB09780511606205.027.
7. Ferziger J. H. and M. Perić. “Turbulent Flows.” *Computational Methods for Fluid Dynamics*. Springer, 2002, pp. 265–307. DOI: 10.1007/978-3-642-56026-2_9.
8. O. C. Zienkiewicz, R. L. Taylor, and P. Nithiarasu. “Turbulent Flows.” *The Finite Element Method for Fluid Dynamics*. 7th ed. Butterworth-Heinemann, 2013. Chap. 8.
9. F. Moukalled, L. Mangani, and M. Darwish. *The Finite Volume Method in Computational Fluid Dynamics: An Advanced Introduction with OpenFOAM® and Matlab*. Fluid Mechanics and Its Applications 113. Springer, 2016. XXIII, 791. DOI: 10.1007/978-3-319-16874-6.
10. S. Rodriguez. *Applied Computational Fluid Dynamics and Turbulence Modeling: Practical Tools, Tips and Techniques*. Springer, 2019. DOI: 10.1007/978-3-030-28691-0.
11. D. A. Anderson, J. C. Tannehill, R. H. Pletcher, M. Ramakanth, and V. Shankar. *Computational Fluid Mechanics and Heat Transfer*. 4th ed. Computational and Physical Processes in Mechanics and Thermal Sciences. CRC Press, 2021. Chap. 5. DOI: 10.1201/9781351124027.
12. L. Brand. “The Pi theorem of dimensional analysis.” *Archive for Rational Mechanics and Analysis*, **1**, (1957), pp. 35–45. DOI: 10.1007/BF00297994.
13. H. L. Langhaar. *Dimensional Analysis and Theory of Models*. John Wiley & Sons, 1951.
14. B. Szabó and I. Babuska. *Introduction to Finite Element Analysis: Formulation, Verification and Validation*. John Wiley & Sons, 2011. DOI: 10.1002/9781119993834.
15. Klaus-Jürgen Bathe. *Finite Element Procedures*. Prentice-Hall, Englewood Cliffs, New Jersey, 1996.
16. Á. G. Pattantyús: *Operation of machines (A gépek üzemtana in Hungarian)*. Műszaki Kiadó, Budapest, 1983. Chap. 3.
17. W. M. Rohsenow, J. R. Hartnett, and Y. I. Cho. *Handbook of Heat Transfer*. 3rd ed. McGraw-Hill, New York, 1998. Chap. 1 and 5. URL: <https://www.accessengineeringlibrary.com/content/book/9780070535558>.
18. F. P. Incropera and D. P. DeWitt. *Fundamentals of Heat and Mass Transfer*. 4th ed. John Wiley & Sons, New York, 1996. Chap. 6.